JOURNAL OF MATERIALS SCIENCE 13 (1978) 253–260

The influence of oxygen and nitrogen on the growth of intermediate phases during the bonding of iron to aluminium

G. M. BEDFORD
Department of Mechanical Engineering and Naval Architecture, Portsmouth Polytechnic, Hampshire, UK

J. BOUSTEAD
Department of Metallurgy and Materials Technology, The North East Wales Institute of Higher Education, Kelsterton College, Clwyd, UK

The reaction between aluminium, and iron containing a range of oxygen and nitrogen up to 0.08% and 0.009% respectively, has been investigated. The kinetics of the early stages of intermediate phase formation have been determined using quantitative metallography, and the results are presented as T–T–T curves. The rate of reaction to form intermediate phases is shown to decrease with increasing oxygen and nitrogen content. In the later stages of intermediate phase growth, the nature and identity of the phases have been established using X-ray diffraction, optical and electron metallography. In the low oxygen and nitrogen specimens a multiphase layer of θ ($FeAl_3$), η (Fe_2Al_5) and ζ ($FeAl_2$) phases develops. In the high oxygen and nitrogen specimens no η (Fe_2Al_5) or ζ ($FeAl_2$) is present, but a thin layer of θ ($FeAl_3$) forms at all temperatures up to 640° C together with the spinel $FeAl_2O_4$ and possibly the oxy-nitride δAl_2O_3/AlN. Simple bend tests indicate that when the layer at the interface consists solely of iron–aluminium intermediate phases the bonding is poor. When the layer is θ ($FeAl_3$) together with ceramic phases as in the high oxygen and nitrogen specimens, bonding is good and the aluminium is still adherent even after 1000 h at 640° C. It is also shown that the accelerating effect of cold work on intermediate phase formation is suppressed by increased oxygen and nitrogen content.

1. Introduction

The bonding of aluminium to iron is important in several industrial processes, for example the manufacture of aluminium composites [1], the friction welding of anode assemblies in aluminium smelters [2], and more widely in protective coatings [3].

In the solid state coating processes, while heat treatment is necessary for a good bond, poor bonding results from excessive heat treatment due to extensive interdiffusion and the formation of a layer of brittle intermediate phases, usually termed "alloy". It is well established that the phases that make up this "alloy" layer, in common with diffusion couples between other partially soluble metals, are those that occur in the equilibrium diagram [4]. Intermediate phases may also form during friction welding unless conditions are carefully controlled. In the hot-dipping process and some methods of composite manufacture [18], the intermediate phases grow as an inherent part of the process, and hence of the bond.

Additions to either aluminium or iron may affect the rate of interdiffusion, leading to increasing complexity of diffusion processes, and possible changes in phase relationships. For example, silicon has been shown to retard the rate

of growth of intermediate phases whether in aluminium [5] or iron [6]. In the hot-dipping process it is established practice to add silicon to the aluminium bath to reduce the rate of thickening of the brittle "alloy" layer.

The effect of oxygen and nitrogen has not been studied extensively, although Canning *et al* [9] and Bullough [10] have indicated the value of a layer of oxide on the iron substrate prior to coating with aluminium. Russian workers [12], however, have recently discussed the role of oxygen in commercial steels clad with aluminium, in terms of the formation of a layer of Al_2O_3 at the interface which inhibits the growth of intermediate phases. Nitrogen has also been observed [10] to limit the growth of intermediate phases, but no explanatory reaction mechanism has been put forward.

In the present work, the role of oxygen and nitrogen on the formation of intermediate phases and subsequent bond strength is discussed in terms of a reaction mechanism involving ceramic phases.

2. Experimental

Vacuum melted iron ingots, containing differing amounts of oxygen and nitrogen, were hot-rolled and finally cold-rolled to 0.9 mm strip. After annealing at 700° C for 3 h in a 95% Ar/5% H_2 atmosphere, the surfaces were prepared for coating by scratch brushing, degreasing in commercial sodium orthosilicate and pickling in 5% HNO_3. High purity and commercial purity aluminium powder were then roll bonded to the strip with a rolling strain of 18 ± 2%, and finally sintered at 390° C for 15 h in a 95% Ar/5% H_2 atmosphere.

Coupons, 25 mm × 10 mm, were cut from the coated strip, heat-treated in a vacuum of 10^{-2} mm Hg at temperatures in the range 500 to 640° C for times up to 1000 h and then quenched into water. Samples for studies of the kinetics of the early stages of alloy growth were heat-treated in a silica tube, evacuated to 10^{-2} mm Hg. The furnace, preset to a given temperature, was drawn along rails over the tube and after the requisite time withdrawn, air admitted into the tube and the samples tipped into water to arrest the reaction. After removal of unreacted aluminium using 10% sodium hydroxide, the progress of the reaction at the iron–aluminium interface, that is, the area of "alloy" coverage, was measured on a quantitative television microscope with an epidiascope attachment at a magnification of 10×.

TABLE I Iron alloys for coating

Code	Carbon (wt %)	Nitrogen (wt %)	Oxygen (wt %)
A	0.004	0.004	0.056
B	0.003	0.007	0.046
C	0.005	0.009	0.082

Typical analysis (wt %) of aluminium powder for coatings:
High purity: 99.99 (Al), 0.005 (Si), 0.005 (Fe).
Commercial purity: 99.74 (Al), 0.07 (Si), 0.15 (Fe), 0.004 (Mn), 0.032 (Zn).

For each series of heat treatments a cross-section and a taper section from the same specimen were prepared for metallographic examination. The taper sections were made by adopting the simple procedure of bending a coupon to approximately 90° and preparing the surface in plan. By this means a section through the coating is achieved at a very acute but indeterminate angle near the bend. Although it is essential to know this angle to calculate the magnification, its magnitude is not vital in this particular application as the technique was adopted merely for the resolution of the constituent phases of the "alloy" layer.

All samples for metallographic examination were ground on paraffin lubricated silicon carbide papers, polished on diamond paste followed by α and then γ alumina. They were etched initially in 2% nital and then in 0.5% HF. Specimens were examined by optical microscopy and in selected cases by electron microscopy using carbon replicas on plastic shadowed with germanium.

Powder for X-ray diffraction was scraped off the specimens after unreacted aluminium had been removed with NaOH. These scrapings were then loaded directly into a glass capilliary without prior sieving. A 114.6 mm diameter Debye–Scherrer powder diffraction camera was used with Co$K\alpha$ radiation at 30 kV 10 mA. A simple bend test was used to indicate bond strength.

3. Results

The nature of "alloy" growth in specimens A and B after removal of unreacted aluminium can be seen in Fig. 1a and b. At these temperatures the low oxygen/nitrogen specimen, A, develops the familiar pattern [7] of discrete islands and preferential edge growth of intermediate phases Fig. 1a. In contrast, the high oxygen/nitrogen specimens, B and C, have an irregular patchy covering which is so thin that it is difficult to obtain enough scrapings for an X-ray photograph.

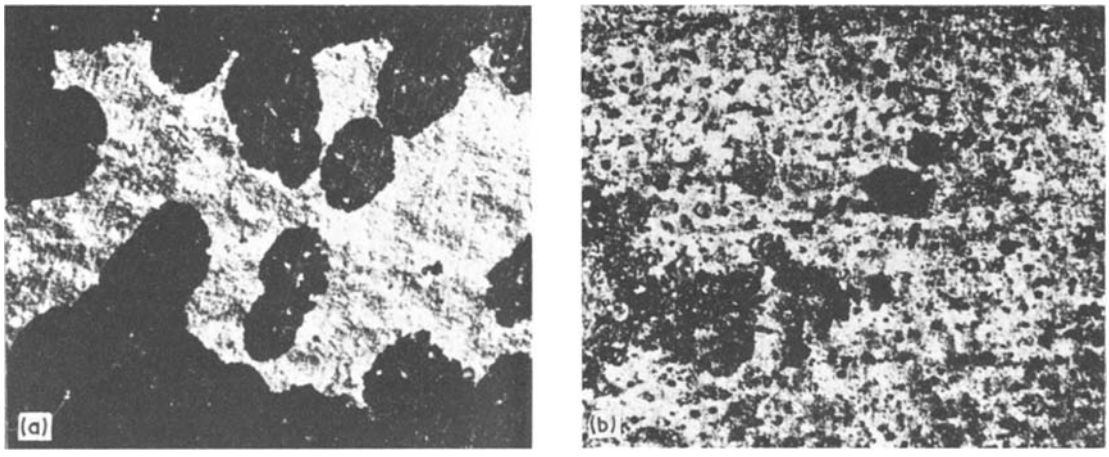

Figure 1 Optical micrograph of plan view of iron interface after chemical removal of aluminium. (a) Specimen A, 80 min at 562° C, showing preferential edge growth, top and botton of the micrograph. (b) Specimen B, 120 h at 551° C; absence of preferential edge growth.

No preferential edge growth is observed in these specimens. Heat treatments in excess of 100 h brought little change in the appearance of this "alloy" layer, Fig. 1b. At temperatures above 560° C the high oxygen/nitrogen specimens develop an "alloy" layer with no preferential edge growth. This layer is black and thick enough to readily obtain scrapings for X-ray photographs.

Values for the T–T–T curves, Fig. 2, were extracted from graphs of percentage transformation versus log time. The percentage transformation represents areas of black "alloy" measured on the Quantimet. As in all nucleation and growth processes, the beginning and end of the transformation cannot be determined precisely, so that 5% to 95% are often taken as the start and finish of the reaction. To determine even these percentages, a large number of specimens are needed to clearly define the tails of the sigmoidal curves of the percentage transformation–time plots from which

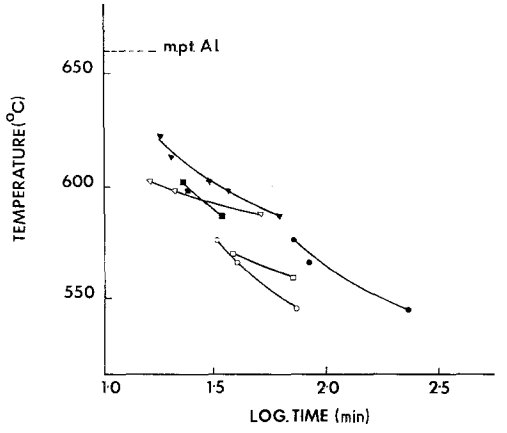

Figure 2 Time–temperature–transformation diagram comparing the rates of "alloy" formation in samples A, B and C, measured as 50% coverage of the iron–aluminium interface. Iron substrate: Specimen A, 0.004% N and 0.056% O, circles; specimen B, 0.007% N and 0.046% O, squares; specimen C 0.009% N and 0.082% O, triangles. Aluminium coating: open symbols, 99.99% pure; shaded symbols, 99.7% pure.

TABLE II X-ray diffraction data from specimen C 480 h at 640° C. CoKα radiation.

Measured		JCPDS	
Intensity*	*d*-spacing (Å)	*d*-spacing (Å)	Phase
vw	4.34		
w	4.07	4.05	θ
w	3.98	3.95	θ
w	3.69	3.68	θ
m	3.53	3.54	θ
w	3.34	3.33	θ
w	3.05	2.95	Fe_2O_3
w	2.52	2.54	$\delta Al_2O_3/AlN$
		2.52	Fe_2O_3
w	2.45	2.48	$\delta Al_2O_3/AlN$
		2.45	$FeAl_2O_4$
m	2.34	2.34	θ
vw	2.27	2.25	θ
vw	2.16	2.16	θ
w	2.11	2.12	θ
m	2.09	2.09	$\theta \cdot Fe_2O_3$
vw	2.05	2.06	θ
s	2.03	2.04	$\theta \cdot FeAl_2O_4$
w	2.00	2.02	$\theta \cdot FeAl_2O_4$
vw	1.95	1.97	$\delta Al_2O_3/AlN$
		1.93	θ
vw	1.81	1.80	θ
w	1.45	1.45	θ
s	1.43	1.43	$\theta \cdot FeAl_2O_4$

*Key: s = strong, m = medium, w = weak, vw = very weak

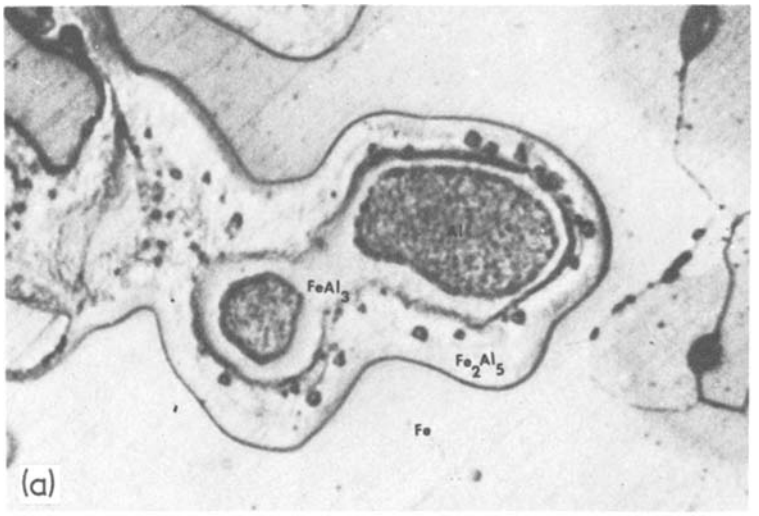

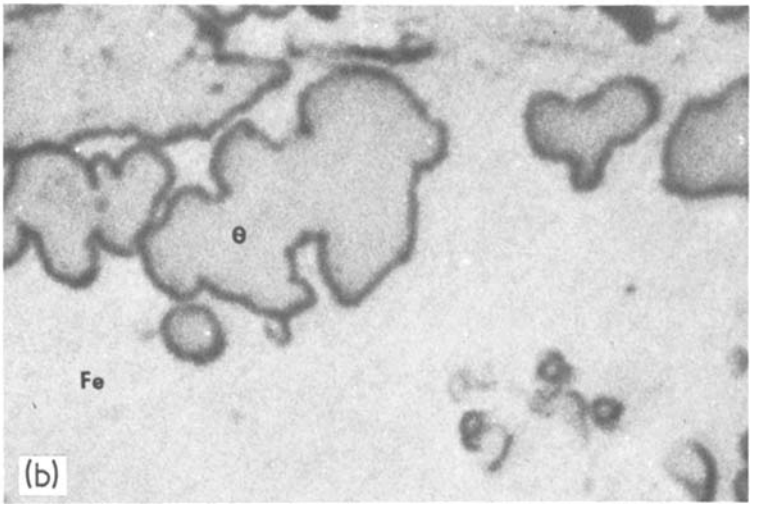

Figure 3 Optical micrographs of taper sections of the iron–aluminium interface; (a) specimen A, multi-phase "alloy" layer, (b) specimen B, single phase "alloy" layer. (× 300).

the T–T–T curves are extracted. In the present investigation the number of specimens was limited, and 50% coverage was chosen to assess the effect of the oxygen/nitrogen additions on the early stages of "alloy" formation prior to thickening. Open points represent samples coated with high-purity and shaded points commercial-purity aluminium. The melting point of aluminium, 660° C, indicates the change from solid state to liquid state reaction.

The *d*-spacings calculated from X-ray diffraction powder photographs of the high oxygen/nitrogen sample, C, heat-treated 480 h at 640° C are listed in Table II. *d*-values (JCPDS) of the $\theta(FeAl_3)$ phase and the spinel, hercynite, $FeAl_2O_4$ are listed. Other lines have only tentatively been accounted for by the phases Fe_2O_3 and δAl_2O_3/AlN. The similarity in their *d*-spacings indicates the need for a focusing camera if the lines are to be resolved. One very weak line, $d = 4.34$ Å, remains unidentified. It is not associated with any of the iron–aluminium intermediate phases.

Optical photomicrographs of a taper section of specimens A and C heat treated for 1000 h at 640° C are shown as Fig. 3a and b. The low oxygen/nitrogen specimen, A, shows the multiphase nature of the "alloy" layer, whereas the high oxygen/nitrogen shows a single phase layer. In the multiphase layer the $\eta(Fe_2Al_5)$ and $\theta(FeAl_3)$ phases were readily identified by X-ray diffraction, but only very faint $\zeta(FeAl_2)$ lines were evident. On Fig. 3a the $\eta(Fe_2Al_5)$ has been located by the presence of a second phase [7] and $\theta(FeAl_3)$ by deduction from its relative position in the equilibrium diagram. No other phase, such as $\zeta(FeAl_2)$, was apparent in the microstructure.

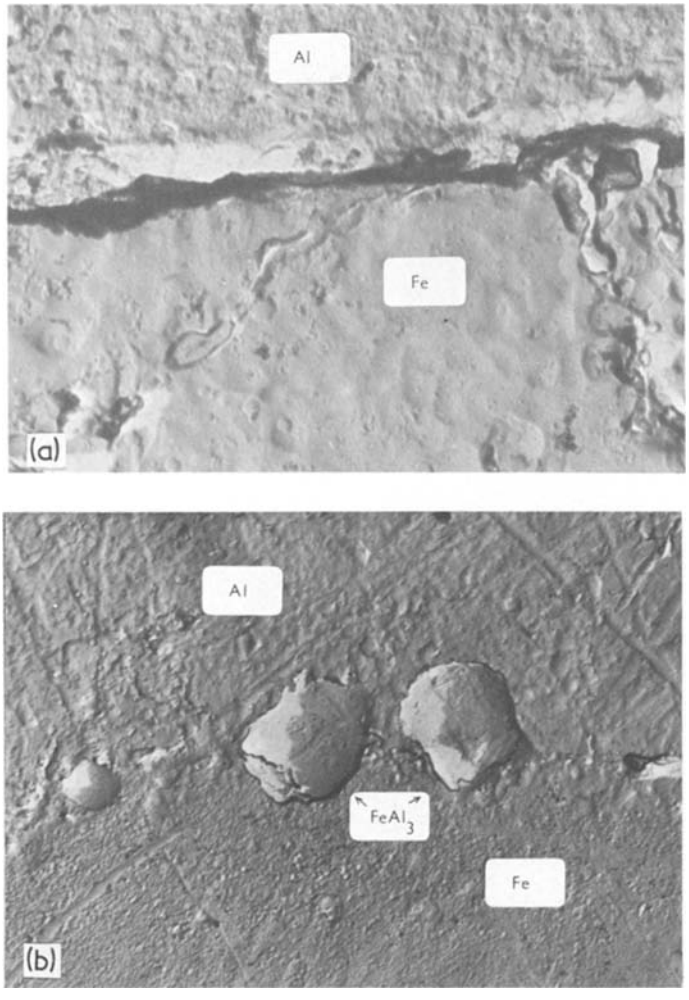

Figure 4 (a) and (b). Carbon replica electron micrographs of a section through specimen B after 240 h at 532° C (× 2970).

Electron micrographs of carbon replicas of specimen B, Fig. 4a and b, illustrate the early stages of the growth of $\theta(FeAl_3)$ at the interface. Growth is very limited except in some parts where it has developed into clearly defined areas. The development of an additional phase only becomes apparent at the higher temperatures, when a thin layer between the aluminium and the $\theta(FeAl_3)$ can be seen, Fig 5. Although there is a distinct interface on the aluminium side of the $\theta(FeAl_3)$ phase, no such distinct boundary is apparent on the iron side. However, in specimen C, Fig. 6, there is a thin layer on the iron side of the $\theta(FeAl_3)$ but only very slight indication of a phase at the aluminium side.

In the bend test on specimen A, heat-treated 1 h at 640° C, the aluminium cracked and became detached after bending through 90°. In contrast, the high oxygen/nitrogen specimens, B and C, heat-treated for 1000 h at 640° C could be bent through 90° with no visible cracking; after bending to 180°, cracking was evident but was not continuous, and the aluminium was still adherent.

4. Discussion

Batz and Thurman [8] have reported on the effect of nitrogen on the formation of iron–aluminium intermediate phases in clad products. The start of intermediate phase growth at the interface, termed "alloying temperature", was obtained for a range of nitrogen concentrations. However, no clear indication was given as to how the "start" of phase growth was defined or measured. "Alloying temperature", like recrystallization

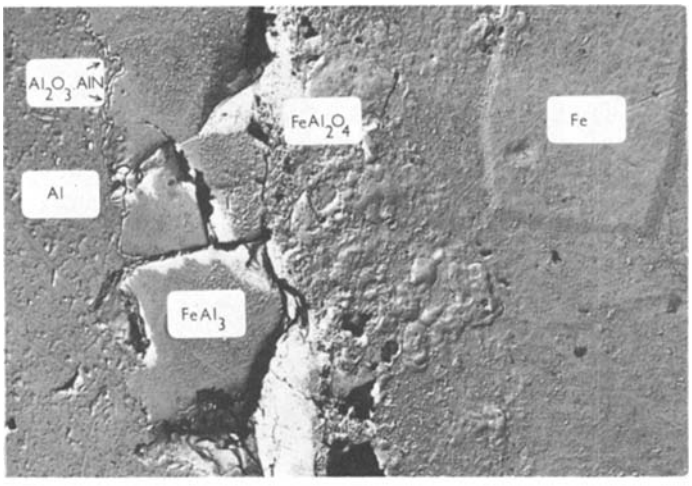

Figure 5 Carbon replica electron micrograph of a section through specimen B after 240 h at 603° C. (× 960).

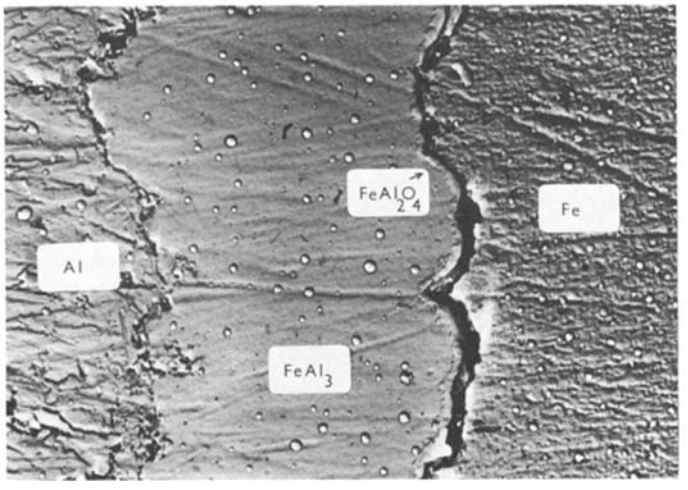

Figure 6 Carbon replica electron micrograph of a section through specimen C after 480 h at 640° C. (× 2600).

temperature, is affected by several variables which preclude simple definition, and the point of part of the present work is to propose a more convenient way of determining the "alloying temperature",. It is defined arbitrarily as 50% coverage of the iron–aluminium interface by intermediate phase growth. Using this method results can be presented in the form of a T–T–T diagram. It must be emphasized that this diagram relates to a stage of intermediate phase growth which predates the build-up of a continuous thick layer of intermediate phases. It is often of particular value to be able to monitor these early stages, particularly in processes where either no "alloy" or only a very thin layer can be tolerated.

The T–T–T diagram obtained, Fig. 2, clearly indicates the effect of increasing oxygen and nitrogen content of the steel, despite the limited number of points. The curve for specimen C is raised by several degrees above the curve for A, and these trends are similar to those observed by Batz and Thurman [8].

The cut edges of the specimens are localized cold-worked areas, which in the low oxygen/nitrogen specimen A exhibit preferential growth of "alloy" in agreement with other workers [13]. In specimen B there is a marked reduction of preferential edge growth and in specimen C it is absent. This is of some interest in industrial processes when it is often necessary to remove cold work, initially used to achieve bonding, to enable further fabrication. The reason for this behaviour is probably associated with a very thin diffusion barrier, which forms even more rapidly in cold-worked areas and prevents development of iron–aluminium intermediate phases. A possible reaction mechanism is discussed later.

The early stages of intermediate phase growth at the interface of sample B is illustrated in Figs. 4a and b. After 240 h at 532° C, no intermediate

phases are visible in the optical microscope, but replicas indicate interface features which may be associated with a reaction product, Fig. 4a. Along the interface there are occasional clusters of well defined areas of the intermediate phase $\theta(FeAl_3)$ Fig. 4b, but no additional phase is apparent. That $\theta(FeAl_3)$ is the first intermediate phase to form between iron and aluminium is an accord with the authors' earlier work [7] and the Mössbauer studies of Preston [17].

At elevated temperatures, 640° C, the low oxygen/nitrogen specimen, A, develops a multiphase "alloy" layer, whereas in the high oxygen/nitrogen specimens, B and C, only $\theta(FeAl_3)$ phase of the iron–aluminium compounds can be identified. There is evidence in the replica micrographs, Fig. 5, specimen B, of a very thin phase which defines clearly the θ/Al boundary. A more diffuse region exists at the θ/Fe interface such that a third phase cannot be excluded. In Fig. 6, specimen C, a thin phase exists at the θ/Fe interface but not at the θ/Al boundary. X-ray diffraction lines in addition to $\theta(FeAl_3)$, and not identified as either $\eta(Fe_2Al_5)$ or $\zeta(FeAl_2)$, have been associated with ceramic phases, notably the spinel, hercynite, $FeAl_2O_4$, and tentatively an oxynitride $\delta\ Al_2O_3/AlN$. It is thought that the phase at the θ/Fe interface is $FeAl_2O_4$, and at the θ/Al interface, $\delta\ Al_2O_3/AlN$.

Popplewell *et al* [11] have shown, using electron microscopy, that the spinel $FeAl_2O_4$ forms readily at an iron oxide/Al_2O_3 interface, even at temperature as low as 450° C. In iron/Al_2O_3 specimens no reaction products were revealed by electron diffraction. However, they did note features in the electron micrographs which could be associated with some reaction having taken place. It is proposed, that in the present work, the identification of the spinel at the interface, implies that the oxygen in the steel forms an oxide of iron, which then reacts with the Al_2O_3 already on the aluminium powder, to form the spinel $FeAl_2O_4$. This is thought to occur prior to any intermediate phase formation which only develops in the high oxygen/nitrogen specimens after extensive heat treatment above about 600° C.

This mechanism differs considerably from recent Russian work [12] in which it is suggested that the oxygen in the steel forms Al_2O_3 at the interface, which then acts as a diffusion barrier inhibiting intermediate phase growth up to 600° C. The Russian workers observed the Al_2O_3 layer to dissolve followed by rapid growth of the intermediate phases. To account for the remarkable stability of the ceramic phases observed in the present investigation, 1000 h at 640° C, it is suggested that the role of the nitrogen is probably to stabilize the Al_2O_3 and/or $FeAl_2O_4$. This is thought to take place by an anion exchange mechanism with oxygen.

The formation of oxynitrides is well documented [13] and lines characteristic of the phase $\delta\ Al_2O_3/AlN$ have been tentatively identified. In the case of the spinel no replacement mechanism of oxygen by nitrogen in ferrospinels is known to the authors, but other anion replacements have been made such that it may be possible for a spinel of the type $FeAl_2O_{4-x}N_x$ to form at the interface.

The enhanced bond strengths observed in the high oxygen/nitrogen specimens, presumably emanate from the presence of the spinel at the interface in the manner well documented for metal–ceramic seals [15, 16]. That is, the oxide phases are strongly adherent to their parent metals, and when in contact at elevated temperatures, undergo a solid-state reaction to form the spinel $FeAl_2O_4$ which effects a strong bond between them. At a later stage, when the aluminium-rich phase $\theta(FeAl_3)$ forms at the aluminium oxide/spinel interface, the bond is maintained. Other authors [9, 10] have reported that the presence of an oxide layer on the iron substrate prior to coating with aluminium improved the bond considerably.

5. Conclusions

Increasing the oxygen and nitrogen content in the iron, up to 0.08% and 0.009% respectively, improves the bond strength between aluminium and iron such that an excellent bond is sustained even after 1000 h at 640° C.

It is proposed that the oxygen in the iron initially forms an iron oxide at the iron aluminium interface, which then reacts with the Al_2O_3 already present to form the spinel $FeAl_2O_4$. The nitrogen is thought to stabilize the Al_2O_3 and/or $FeAl_2O_4$ by undergoing anion replacement to form $\delta\ Al_2O_3/AlN$ and/or $FeAl_2O_{4-x}N_x$.

Growth of the iron–aluminium intermediate phases is limited by this diffusion barrier, and in the high oxygen/nitrogen specimens only a thin layer of $\theta(FeAl_3)$ forms even after 1000 h at 640° C. In the low oxygen/nitrogen samples no ceramic phases are observed, only a multiphase

layer of the iron–aluminium compounds $\zeta(FeAl_2)$, $\eta(Fe_2Al_5)$ and $\theta(FeAl_3)$ which results in a very poor bond.

The effect of cold work on "alloy" growth is thought to be suppressed in the high oxygen/nitrogen samples by the rapid growth of the ceramic phases, which form a diffusion barrier to intermediate phase growth.

Acknowledgements

The authors wish to thank Mr E. W Williams, BSC, Shotwick, for his interest and helpful discussions, and Professor K. M. Entwistle for kindly allowing use of the electron-optical instruments at the Department of Metallurgy, University of Manchester Institute of Science and Technology. They are grateful to Mr I. Brough, Mrs S. Blain and Mr A. C. Steele for their help in the operation of these instruments. The financial support for this work was provided in the form of a grant by the BSC.

References

1. I. N. ARCHANGELSKA and S. T. MILEIKO, *J. Mater. Sci.* **11** (1976) 356.
2. C. R. G. ELLIS and D. BALL, *Met. Constr. and Brit. Weld. J.* October (1970) 447.
3. S. L. CASE and K. R. VAN HORN, "Aluminium in Iron and Steel" (J. Wiley, New York, 1953).
4. J. S. KIRKALDY *Can. J. Physics,* **36** (1958) 899.
5. D. O. GITTINGS, D. H. ROWLAND and J. D. MACK, *Trans. ASM,* **43** (1951) 587.
6. G. M. BEDFORD and J. BOUSTEAD, *Metals Technology* May (1974) 249.
7. *Idem, ibid,* May (1974) 233.
8. W. BATZ and J. W. THURMAN: US Patent, 2 965 963, "Aluminium Cladding of Steel", December 27th 1960.
9. T. A. CANNING, I. DAVIES, and W. M. GIBBON, *JISI,* **205** (1967) 848.
10. W. BULLOUGH, *ibid* **205** (1967) 6.
11. J. M. POPPLEWELL, T. G. CARRUTHERS and J. NUTTING, *ibid* **205** (1967) 8.
12. M. S. MAKUNIN, V. I. ZHELADNOV, P. M. ARZHANYI, M. A. BENYAKOVSKII, A. T. TAT' YANSHCHIKOV, S. Z. RAKAVICH and V. P. BEKHELEV, *Stal* **5** (1974), 407.
13. A. M. LEJUS, *Bull. Soc. Chim. Fr.* **11/12** (1962) 2123.
14. T. HEUMANN and S. DITTRICH, *Z. Metallk.* **50** (1969) 617.
15. A. G. PINCUS, *J. Amer. Ceram. Soc.* **36** (5) (1953) 152.
16. E. P. DENTON and H. RAWSON, *J. Brit. Ceram. Soc.* **59** (1960) 25.
17. R. S. PRESTON, *Met. Trans.* **3** (1972) 1831.
18. E. FRIEDRICH, W. POMPE and I. M. KOPJOV. *J. Mater. Sci.* **9** (1974) 1911.

Received 21 February and accepted 6 May 1977.